

# Effects of Mixed Solvents and PVDF Types on Performances of PVDF Microporous Membranes

Qian Li,<sup>1,2</sup> Zhen-Liang Xu,<sup>1,2</sup> Li-Yun Yu<sup>2</sup>

<sup>1</sup>State Key Laboratory of Chemical Engineering, East China University of Science and Technology (ECUST), Shanghai 200237, China

<sup>2</sup>Membrane Science and Engineering R&D Lab, Chemical Engineering Research Center, ECUST, Shanghai 200237, China

Received 2 April 2009; accepted 23 August 2009

DOI 10.1002/app.31324

Published online 7 October 2009 in Wiley InterScience (www.interscience.wiley.com).

**ABSTRACT:** Polyvinylidene fluoride (PVDF) microporous flat membranes were cast with different kinds of PVDFs and four mixed solvents [trimethyl phosphate (TMP)-*N,N*-dimethylacetamide (DMAc), triethyl phosphate (TEP)-DMAc, tricresyl phosphate (TCP)-DMAc, and tri-*n*-butyl phosphate (TBP)-DMAc]. The effects of different commercial PVDFs (Solef<sup>®</sup> 1015, FR 904, Kynar 761, Kynar 741, Kynar 2801) on membrane morphologies and membrane performances of PVDF/TEP-DMAc/PEG200 system were investigated. The membrane morphologies were examined by scanning electron microscopy (SEM). The membrane performances in terms of pure water flux, rejection, porosity, and mean pore radius were measured. The membrane had the high flux of  $143.0 \pm 0.9 \text{ L m}^{-2} \text{ h}^{-1}$  when the content of TMP in the TMP-DMAc mixed solvent reached 60 wt %, which was 2.89 times that of the membrane cast with DMAc as single solvent and was 3.36 times that of the membrane cast with TMP as single solvent. Using mixed solvent with different solvent solubility parameters, different morpholo-

gies of PVDF microporous membranes were obtained. TMP-DMAc mixed solvent and TEP-DMAc mixed solvent indicated the stronger solvent power to PVDF due to the lower solubility parameter difference of  $1.45 \text{ MPa}^{1/2}$  and the prepared membranes showed the faster precipitation rate and the higher flux. The less macrovoids of the membrane prepared with TEP (60 wt %)-DMAc (40 wt %) as mixed solvent contributed to the higher elongation ratio of  $96.61\% \pm 0.41\%$ . Therefore, using TEP(60 wt %)-DMAc (40 wt %) as mixed solvent, the casting solution had the better solvent power to PVDF, and the membrane possessed the excellent mechanical property. The microporous membranes prepared from casting solutions with different commercial PVDFs exhibited similar morphology, but the water flux increased with the increment of polymer solution viscosity. © 2009 Wiley Periodicals, Inc. *J Appl Polym Sci* 115: 2277–2287, 2010

**Key words:** polyvinylidene fluoride; mixed solvent; precipitation rate; microporous flat membrane

## INTRODUCTION

Membrane techniques have been extensively used in separation facilities to separate liquid/liquid or liquid/solid mixture.<sup>1</sup> Polyvinylidene fluoride (PVDF) is regarded as one of the most attractive polymer materials in microporous membrane industry. The molecular structure of PVDF homopolymer with alternating CH<sub>2</sub> and CF<sub>2</sub> groups along the polymer chain forms a unique polymer with some of the best characteristic of polyethylene combined with performance approaching polytetrafluoroethylene.<sup>2</sup> It provides extraordinary mechanical properties, high chemical resistance, good thermal stability and excellent biocompatibility.<sup>3</sup> Therefore, PVDF is a suitable material to make membrane, which has been applied

in lithiumion batteries, piezoelectric sensors, pervaporation or film filtration, protein purification, bacteria filtration, water-treatment applications, gas separation, petrochemical industry, and so on.<sup>4–9</sup>

PVDF microporous flat membranes are frequently prepared via nonsolvent inversion separation (NIPS), that is, casting solution is immersed into a nonsolvent coagulation bath to induce a series of liquid–solid and/or liquid–liquid phase separation events.<sup>10</sup> However, as one of the semicrystalline polymers, PVDF has been reported to exhibit more complicated phase separation behavior than amorphous polymers in this process, which actually provides more freedom to optimize membrane properties.<sup>11</sup> Many formation parameters affect polymer precipitation and ultimately the morphology of the formed PVDF microporous membranes. In fact, the amount of solvent in the polymeric membrane greatly influences the membrane morphology. Yeow et al.<sup>12</sup> compared the morphology of PVDF membranes with different solvent systems, including 1-methyl-2-pyrrolidone (NMP), *N,N*-dimethylformamide (DMF), *N,N*-dimethylacetamide (DMAc), and triethyl phosphate (TEP). The results revealed the

Correspondence to: Z.-L. Xu (chemxuzl@ecust.edu.cn).

Contract grant sponsor: National “Eleventh Five-Year” Important Science and Technology Supporting Plan; contract grant number: 2006BAE02A01.

distinctive influences of various solvents on membrane structures, indicating the importance of the solvent. Applying a two-phase flow consisting of a solvent and a dope solution in the air gap region of spinning through a NIPS process, Bonyadi and Chung<sup>13</sup> fabricated highly porous and macrovoid-free PVDF hollow fiber membranes. Besides, The effect of PVDF concentration on membrane morphology and crystal forms was discussed by Buonomenna.<sup>14</sup> Recently, Zhang showed that higher PVDF concentration in casting solution yielded the membrane with higher crystallinity and higher  $\beta/\alpha$  phase ratio in the surface layers.<sup>3</sup> In fact, with the proper selection, a desired membrane structure and satisfactory membrane separation performance can be anticipated.<sup>15–23</sup>

DMAc and phosphates [trimethyl phosphate (TMP) and TEP] are good solvents for PVDF, and DMAc demonstrates a stronger solvent power to PVDF. When TMP or DMAc is used as solvent, PVDF membrane exhibits the finger-like structure. Nevertheless, the flat sheet membranes cast with TEP as solvent exhibits symmetry sponge structure. Therefore, using phosphate–DMAc mixture as solvent, the solvent power to PVDF membrane can be improved, as well as membrane morphology can be controlled. On the other hand, it is impossible that all commercial PVDFs possess identical properties. The chemical and physical properties of different PVDFs also influence the membrane performances. However, the phosphate–DMAc mixed solvent has been rarely used in the casting solution, and few studies have focused on comparing the effects of different commercial PVDFs. The purpose of this study was to systematically investigate the effects of four different mixed solvents [TMP–DMAc, TEP–DMAc, tricresyl phosphate (TCP)–DMAc and tri-*n*-butyl phosphate (TBP)–DMAc] and different PVDFs (Solef<sup>®</sup> 1015, FR 904, Kynar 761, Kynar 741, Kynar 2801) on the membrane morphologies and performances. The performances of PVDF (Solef<sup>®</sup> 1015) microporous membranes cast with different content of TMP in the mixed solvent (TMP–DMAc) were compared. An improved self-made transmittance device was used to test the precipitation rate during the immersion process. The morphologies of the membranes were investigated by scanning electron microscopy (SEM).

## EXPERIMENTAL

### Materials

Solef<sup>®</sup> 1015 PVDF and FR 904 PVDF were purchased from Solvay Advanced Polymers, L.L.C. (Alpharetta, GA, USA) and Shanghai 3F New Materials (PR China), respectively. Kynar 761 PVDF, Kynar 741 PVDF and Kynar 2801 PVDF were purchased from Arkema (France). DMAc and TBP produced by

Shanghai Lingfeng Chemical Reagent Corporation (PR China). TMP, TEP, TCP, and polyethylene glycol (PEG200) purchased from Sinopharm Chemical Reagent (PR China).

### Determination of coagulation value

Coagulation value (CV) can be used as a measurement of the thermodynamic stability of the casting solution system. 100 g of PVDF (15 wt %)/mixed solvent/PEG200 (5 wt %) casting solution was kept at 25°C and H<sub>2</sub>O as the nonsolvent was slowly added dropwise. Every drop caused local coagulation and further addition was carried out only after the casting solution became homogeneous again. When the addition solution caused remarkable coagulation and the coagulation was not dissolved at 25°C in 24 h, CV is designed by the addition amount of H<sub>2</sub>O in grams required to make 100 g polymer solution turbid.

### Light transmittance measurement

Light transmittance measurement experiment was carried by a self-made device as described by Li et al.<sup>1</sup> A collimated laser was directed on the glass plate immersed in the coagulation bath. The light intensity information was captured by the light detector and then recorded in the computer. The precipitation rate of the casting solution in the coagulation bath could be characterized by the curve of light transmittance to immersion time.

### Membrane casting

The microporous flat PVDF membranes were prepared via NIPS process. PVDF powders (15 wt %) and the additive (5 wt % PEG200) were added to the mixed solvent (TMP–DMAc, TEP–DMAc, TCP–DMAc, TBP–DMAc) in a triangle beaker, and the solutions were mechanically stirred for at least 24 h to guarantee complete dissolution of the polymer at 70–90°C. The casting solutions were cast onto a glass plate at 25°C and 60%  $\pm$  5% relative humidity by means of a casting knife with a gap of 380  $\mu$ m, and then were immersed into a coagulation bath (deionized water at 25°C) after 30 s of evaporation time. After complete coagulation, the membranes were transferred into a fresh water bath, which was refreshed frequently, to remove the traces of the residual solvent, and then the prepared membranes were kept in deionized water until used. The components for various membranes are summarized in Table I.

### Membrane characterization

PVDF microporous membranes were characterized by determination of pure water flux ( $J$ ), rejection ( $R$ ), porosity ( $\epsilon$ ), and mean pore radius ( $r_m$ ).

TABLE I  
Membranes Cast with Different Components

Membrane	Polymer (PVDF)	Solvent (wt %)				
		DMAc	TMP	TEP	TCP	TBP
MTMP0	Solef 1015	100	0	–	–	–
MTMP20	Solef 1015	80	20	–	–	–
MTMP40	Solef 1015	60	40	–	–	–
MTMP60	Solef 1015	40	60	–	–	–
MTMP80	Solef 1015	20	80	–	–	–
MTMP100	Solef 1015	0	100	–	–	–
MTEP60	Solef 1015	40	–	60	–	–
MTCP60	Solef 1015	40	–	–	60	–
MTBP60	Solef 1015	40	–	–	–	60
MTEP60-A	FR 904	40	–	60	–	–
MTEP60-B	Kynar 761	40	–	60	–	–
MTEP60-C	Kynar 741	40	–	60	–	–
MTEP60-D	Kynar 2801	40	–	60	–	–

A self-made dead end stirred-cell was used to measure the pure water flux of the PVDF membranes and the rejection test was carried out with an aqueous solution of bovine serum albumin (BSA,  $M_W = 67000$ ,  $300 \text{ mg L}^{-1}$ ). All experiments were conducted at room temperature ( $25^\circ\text{C}$ ) and at a constant operation pressure of  $0.1 \text{ MPa}$ . The pure water flux and the rejection are defined as formulae (1) and (2), respectively.

$$J = \frac{Q}{A \times T} \quad (1)$$

$$R = \left(1 - \frac{C_P}{C_F}\right) \times 100\% \quad (2)$$

where  $J$  is the water flux ( $\text{L h}^{-1} \text{ m}^{-2}$ ),  $Q$  is the volume of the permeate pure water ( $L$ ),  $A$  is the effective area of the membrane ( $\text{m}^2$ ), and  $T$  is the permeation time (h).  $R$  is the rejection to BSA (%),  $C_P$  and  $C_F$  are the permeate and feed concentration, respectively (wt %).

The membrane porosity  $\varepsilon$  (%) is defined as the volume of the pores divided by the total volume of the microporous membrane. It can usually be determined by gravimetric method, determining the weight of liquid (here, pure water) contained in the membrane pores.<sup>24</sup>

$$\varepsilon = \frac{(m_1 - m_2)/\rho_w}{(m_1 - m_2)/\rho_w + m_2/\rho_p} \quad (3)$$

where  $m_1$  is the weight of the wet membrane (g);  $m_2$  is the weight of the dry membrane (g);  $\rho_w$  is the water density ( $0.998 \text{ g cm}^{-3}$ ) and  $\rho_p$  is the polymer density ( $1.778 \text{ g cm}^{-3}$ ).

The membrane thickness was determined by an electronic digital caliper (Shanghai, Shenhan). The mean pore radius is determined by filtration velocity

method. According to Guerout-Elford-Ferry equation,  $r_m$  ( $\mu\text{m}$ ) can be calculated:<sup>25</sup>

$$r_m = \sqrt{\frac{(2.9 - 1.75\varepsilon) \times 8\eta l q}{\varepsilon \times A \times \Delta P}} \quad (4)$$

where  $\eta$  is water viscosity ( $8.9 \times 10^{-4} \text{ Pa s}$ );  $l$  is the membrane thickness (m);  $q$  is the volume of the permeate water per unit time ( $\text{m}^3 \text{ s}^{-1}$ ),  $A$  is the effective area of the membrane ( $\text{m}^2$ ), and  $\Delta P$  is the operation pressure ( $0.1 \text{ MPa}$ ).

All the data are presented with the standard deviation.

### Measurement of solution viscosity

Viscosities of PVDF solutions with different mixed solvents and different PVDF types were measured using a Rheometer Measuring System (Physica MCR101) at  $25^\circ\text{C}$ . This equipment uses the ramp stress test method, whereby a gradually increasing ramped stress was applied onto the sample solution, and the induced shear rate was continuously monitored. The viscosity of the sample solution was calculated, based on the ratio of the two parameters (i.e., shear stress versus shear rate). The report data was the viscosity at a shear rate of  $10 \text{ s}^{-1}$ .

### Mechanical property

Tensile strength (MPa) and elongation ratio (%) were measured by material test-machine (Zwick Z010, Germany) at a loading velocity of  $50 \text{ mm min}^{-1}$ . The report data were the average value of five experimental runs.

### Morphology observation

The morphologies of the top surface (defined as the surface contacting with the coagulation bath), the

TABLE II  
Solubility Parameters of Polymer, Solvents, and Additive

Components	$\delta_d$ (MPa <sup>1/2</sup> )	$\delta_p$ (MPa <sup>1/2</sup> )	$\delta_h$ (MPa <sup>1/2</sup> )	$\delta_t$ (MPa <sup>1/2</sup> )	$\rho$ (g cm <sup>-3</sup> )	$M$ (g mol <sup>-1</sup> )	$V$ (cm <sup>3</sup> mol <sup>-1</sup> )
PVDF	17.2	12.5	9.2	23.17	–	–	–
DMAc	16.8	11.5	10.2	22.77	0.94	87.12	92.40
TMP	16.8	16.0	10.2	25.34	1.97	140.08	71.11
TEP	16.8	11.5	9.2	22.34	1.07	182.15	170.23
TCP	19.0	12.3	4.5	23.08	1.17	368.00	314.53
TBP	16.4	6.3	4.3	18.09	0.98	266.32	271.76
PEG200	16.7	7.6	14.5	23.39	1.13	200.00	177.78

bottom surface (the surface contacting with the glass plate), and the cross-section of the sample membranes were examined by SEM using a JEOL Model JSM-6360LV SEM (Tokyo, Japan). Before experiments, all the samples of the membranes were frozen in liquid nitrogen, then broken and deposited on a copper holder. Cross-section and surface of the membranes were sputtered with gold and then transferred to the microscope.

### Calculation of solubility parameters

The basis of Hansen solubility parameters is a division of the cohesion energy of volatile liquids into three parts:  $\delta_d$ ,  $\delta_p$ , and  $\delta_h$ . All of the cohesive bonds holding the liquid together were broken when it evaporated. The three Hansen solubility parameters quantitatively represent the nonpolar (atomic) bonding ( $d$ ), the permanent dipole–permanent dipole (molecular) bonding ( $p$ ), and the hydrogen (molecular) bonding ( $h$ ), respectively.<sup>26–31</sup>

$$\delta_i^2 = \delta_d^2 + \delta_p^2 + \delta_h^2 \quad (5)$$

where  $\delta_d$ ,  $\delta_p$ , and  $\delta_h$  are the Hansen solubility parameters (MPa<sup>1/2</sup>).  $\delta_d$  is found from corresponding states principles at 25°C,  $\delta_p$  is found with the aid of dipole moments and other parameters, and  $\delta_h$  is usually found by what is left over in eq. (5) or by group contributions.

The solubility parameter of additive-solvent is giving by the following equation.<sup>32</sup>

$$\delta_{i,s} = \frac{X_1 V_1 \delta_{i,1} + X_2 V_2 \delta_{i,2}}{X_1 V_1 + X_2 V_2}, i = d, p, h \quad (6)$$

where  $X$  is the molar fraction,  $V$  is the molar volume (cm<sup>3</sup> mol<sup>-1</sup>), subscript 1 is the solvent and 2 is the additive,  $d$ ,  $p$ ,  $h$  are ditto.

And the difference of solubility parameters between additive-solvent and polymer can be described as:<sup>32</sup>

$$\Delta\delta_{s-p} = \left[ (\delta_{d,s} - \delta_{d,p})^2 + (\delta_{p,s} - \delta_{p,p})^2 + (\delta_{h,s} - \delta_{h,p})^2 \right]^{0.5} \quad (7)$$

where  $\delta_{i,s(i=d,p,h)}$  are the Hansen solubility parameters of additive-solvent;  $\delta_{i,p(i=d,p,h)}$  are the Hansen solubility parameters of polymer,<sup>33</sup> which are listed in Table II.

## RESULTS AND DISCUSSION

### Effect of TMP content in the mixed solvent on membrane performance

Solvent plays an important role in preparing polymer membranes via NIPS process. It highly influences whether the polymer solution can remain uniform or stable. DMAc is a good solvent for PVDF.<sup>12</sup> By mixing TMP and DMAc as solvent, PEG200 used as additive, the effects of TMP content in the mixed solvent on the membrane morphologies and performances were investigated.

The light transmittance curves of the casting solution are shown in Figure 1, which illustrated that the precipitation process includes two stages at lower TMP content (MTMP0, MTMP20, and MTMP40), in the first stage, the light transmittance decreases slowly; in the second stage, the light transmittance decreases quickly at first and then reduces slowly till changeless at last. At 0, 20, and 40 wt %, the first stage lasts about 45, 35, and 30s, respectively; the

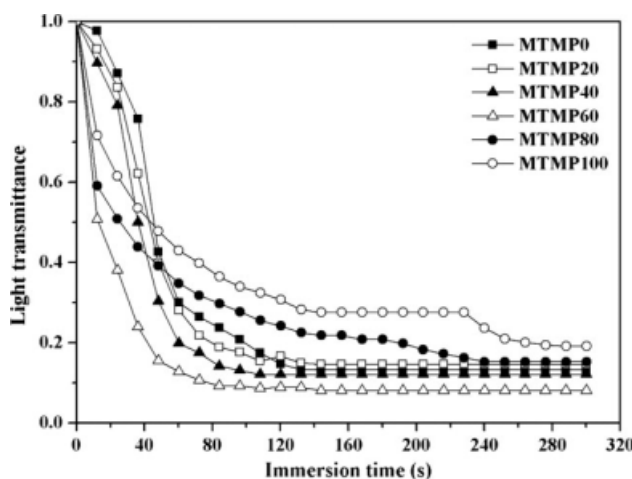
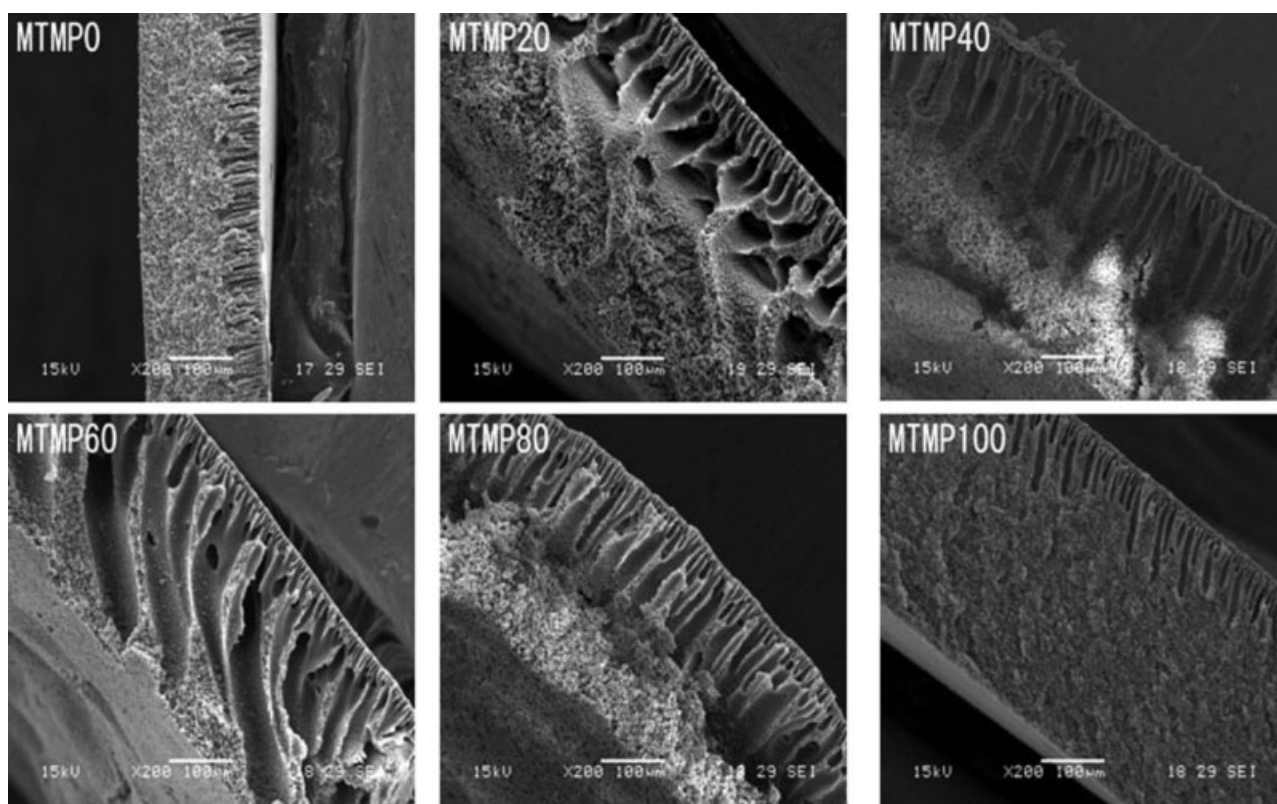


Figure 1 Light transmittance during immersion of casting solutions with different TMP content in the TMP–DMAc mixed solvent.



**Figure 2** SEM pictures of the cross-section morphologies of PVDF microporous membranes prepared by casting solutions with different TMP content in the TMP-DMAC mixed solvent.

period of the first stage finally decreases as the content of TMP in the mixed solvent increases from 0 to 40 wt %. For the membrane with higher TMP content (MTMP60, MTMP80, and MTMP100), the light transmittance decreases quickly in a few seconds after the membrane was immersed into the coagulation bath, and the precipitation rate decreases with the increase of TMP content from 60 to 100 wt %. Therefore, the precipitation rate is the fastest during immersion process with 60 wt % TMP in the mixed solvent, which favors the formation of a finger-like membrane structure.

Figure 2 shows that underneath the skin is a region composed of parallel finger-like macrovoids and finally the lower part of the membrane cross-section shows cellular pores at lower TMP content (MTMP0, MTMP20, MTMP40). In fact, these finger-like voids lengthened with the increase of TMP content from 0 to 60 wt % (MTMP0 to MTMP60) but then shortened as the content of TMP further increased from 60 to 100 wt % (MTMP60 to MTMP100). That is, due to the faster rate of precipitation, adding 60 wt % of TMP to the mixed solvent, the macrovoids, which are larger elongated pores, extend over the entire membrane thickness and become longest.

It has been generally accepted that the morphology of microporous membrane affected by the precipitation rate influences the performances of the membrane. As shown in Table III, the flux and the porosity of the membrane cast with TMP (60 wt %)-DMAC (40 wt %) (MTMP60) are maximized, which are  $143.0 \pm 0.9 \text{ L m}^{-2} \text{ h}^{-1}$  and  $81.8\% \pm 0.2\%$ , respectively. The flux of the membrane prepared with using TMP (60 wt %)-DMAC (40 wt %) as solvent (MTMP60) is 2.89 times that of the membrane cast with DMAC as single solvent (MTMP0) and is 3.36 times that of the membrane cast with TMP as single solvent (MTMP100). According to the aforementioned experiment results, the growing of macrovoids decreases permeation resistance and leads to the higher flux and porosity. However, the rejection of MTMP60 is approaching to that of others (MTMP0, MTMP20, MTMP40, MTMP80, and MTMP100), all around 75%; this result can be explained by the existence of macrovoids beneath the skin layer in all of the cross-section morphologies.

Therefore, the addition of 60 wt % of phosphate in the mixed solvent is used in our further investigation on the effects of different mixed solvent on the membrane morphology and performances, as discussed in the following investigations.

**TABLE III**  
Performances of PVDF Microporous Membranes

Membrane	$J$ ( $L m^{-2} h^{-1}$ )	$R$ (%)	$\varepsilon$ (%)	$r_m$ ( $\mu m$ )
MTMP0	$49.5 \pm 0.2$	$75.7 \pm 0.2$	$76.3 \pm 0.2$	$0.022 \pm 0.001$
MTMP20	$51.5 \pm 0.3$	$76.2 \pm 0.3$	$79.9 \pm 0.3$	$0.025 \pm 0.001$
MTMP40	$67.2 \pm 0.5$	$76.9 \pm 0.1$	$80.5 \pm 0.1$	$0.027 \pm 0.001$
MTMP60	$143.0 \pm 0.9$	$73.8 \pm 0.3$	$81.8 \pm 0.2$	$0.040 \pm 0.002$
MTMP80	$69.5 \pm 0.5$	$77.2 \pm 0.2$	$80.5 \pm 0.2$	$0.028 \pm 0.001$
MTMP100	$42.5 \pm 0.3$	$78.0 \pm 0.2$	$79.6 \pm 0.1$	$0.022 \pm 0.001$
MTEP60	$64.6 \pm 0.2$	$90.1 \pm 0.4$	$76.1 \pm 0.2$	$0.026 \pm 0.001$
MTCP60	$42.7 \pm 0.4$	$80.2 \pm 0.1$	$67.2 \pm 0.2$	$0.024 \pm 0.001$
MTBP60	$19.1 \pm 0.3$	$78.5 \pm 0.2$	$47.4 \pm 0.1$	$0.020 \pm 0.001$
MTEP60-A	$28.3 \pm 0.2$	$90.6 \pm 0.1$	$77.2 \pm 0.3$	$0.019 \pm 0.001$
MTEP60-B	$23.4 \pm 0.3$	$90.5 \pm 0.1$	$80.1 \pm 0.2$	$0.017 \pm 0.001$
MTEP60-C	$21.8 \pm 0.4$	$91.4 \pm 0.1$	$81.4 \pm 0.2$	$0.016 \pm 0.001$
MTEP60-D	$14.9 \pm 0.2$	$91.2 \pm 0.1$	$82.2 \pm 0.3$	$0.014 \pm 0.001$

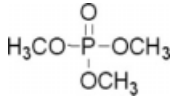
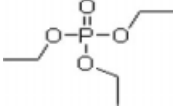
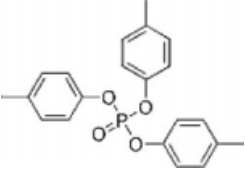
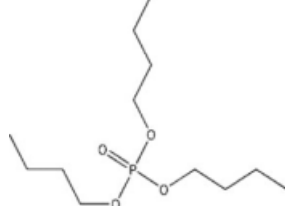
### Effect of different phosphates in the mixed solvent on membrane performance

Using water as coagulant and PEG200 as additive, four phosphate solvents (TMP, TEP, TCP, and TBP) of 60 wt % were mixed with DMAc of 40 wt % respectively, to study the morphologies of PVDF microporous flat membranes prepared by NIPS process.

If the solubility parameter of polymer is consistent with that of a solvent, the solvent demonstrates the strong solvent power to polymer in theory.<sup>27</sup> Therefore, the low solubility parameter difference between additive-solvent system and PVDF ( $\Delta\delta_{s-p} < 2MPa^{1/2}$ )

indicates the strong solvent power of additive-solvent system to PVDF. As shown in Table IV, for MTMP60 and MTEP60, the solvent showed the stronger power to PVDF due to the lower solubility parameter difference of  $1.45 MPa^{1/2}$ . And the TBP-DMAc (MTBP60) is the poorest solvent because of the highest solubility parameter difference ( $\Delta\delta_{s-p} = 4.66 MPa^{1/2}$ ). On the other hand, the substituent size in four phosphate molecule follows the order of  $TMP < TEP < TCP < TBP$ . Due to the steric effect and molecular interaction,<sup>34</sup> the solvent power of four solvents to PVDF follows the order of  $TMP > TEP > TCP > TBP$ .

**TABLE IV**  
Properties of Different Casting Solutions and the Prepared Membranes

Membrane	Phosphate molecular structure	$\Delta\delta_{s-p}$ ( $MPa^{1/2}$ )	Coagulation value (g)	Viscosity (cp)	Thickness ( $\mu m$ )
MTMP60		1.45	$3.90 \pm 0.08$	$6780 \pm 50$	$330 \pm 0.5$
MTEP60		1.45	$3.53 \pm 0.06$	$7310 \pm 46$	$297 \pm 0.6$
MTCP60		2.02	$2.69 \pm 0.04$	$16200 \pm 62$	$280 \pm 0.4$
MTBP60		4.66	$1.93 \pm 0.05$	$24300 \pm 85$	$235 \pm 0.6$

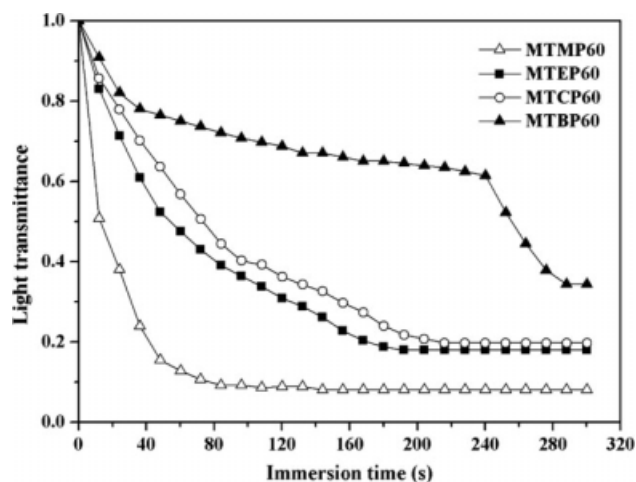


**Figure 3** Light transmittance during immersion of casting solutions with different phosphate–DMAc mixed solvent.

In addition, CV was used to measure the thermodynamic stability of different casting solutions. The results are listed in Table IV. The CV follows the trend of MTMP60 ( $3.90 \pm 0.08$  g) > MTEP60 ( $3.53 \pm 0.06$  g) > MTCP60 ( $2.69 \pm 0.04$  g) > MTBP60 ( $1.93 \pm 0.05$  g). It means that the casting solution of MTCP60 and MTBP60 were thermodynamically less stable. It is well agreed with the prediction by the solubility parameters.

Viscosity has a strong influence on the interdiffusion of solvent and nonsolvent during the immersion precipitation process, which then controls the kinetic aspect of membrane formation process, including both skin formation and substructure morphology.<sup>34</sup> As shown in Table IV, the viscosities of 15 wt % PVDF casting solutions prepared with different mixed solvent, TMP–DMAc (MTMP60), TEP–DMAc (MTEP60), TCP–DMAc (MTCP60), TBP–DMAc (MTBP60), follow the order of MTBP60 > MTCP60 > MTEP60 > MTMP60, which is consistent with the trend followed by the solubility parameter difference. That is, the weaker solvent power due to the higher solubility parameter difference between additive–solvent system and PVDF results in the higher viscosity.

The light transmittance curves shown in Figure 3 reveal that the precipitation rate follows the trend of MTMP60 > MTEP60 > MTCP60 > MTBP60, which is inversely proportional to the casting solution viscosity (MTBP60 > MTCP60 > MTEP60 > MTMP60). In the case of TBP–DMAc (MTBP60), due to the poor solvent power, the precipitation process shows a delayed demixing, including two stages; moreover, the first stage lasts as long as 240 s; this indicates a quite slow precipitation process in the cross-section, which hinders the development of finger-like voids. Compared to MTBP60, the precipitation processes of

MTCP60 and MTEP60 are slightly faster. The phase inversion process of the casting solution using TMP–DMAc as mixed solvent (MTMP60) is the fastest of the four, and therefore, the finger-like voids can develop completely.

Figure 4 shows that PVDF microporous membranes cast with TBP–DMAc (MTBP60) and TCP–DMAc (MTCP60) exhibit a similar sponge structure through the whole thickness with a dense and wizened surface. Because of the weak solvent power, which has been mentioned earlier, the minority presence of the nonsolvent (water) is sufficient to induce the phase inversion of the polymer solution; therefore, the macrovoids cannot develop. The membrane with TEP–DMAc as solvent (MTEP60) shows a short finger-like structure with sponge substrates, which suggests the formation of a skin layer at an early stage; this favors the formation of a finger-like membrane structure. In the case of TMP–DMAc as solvents (MTMP60), long finger-like voids extending toward the bottom region are observed beneath the skin layer. This structure indicates a fast precipitation rate during the immersion process, which agrees with the result of light transmittance experiment. In addition, the bottom surface of MTEP60 is slightly less porous than that of MTMP60, but compared to MTCP60 and MTBP60, the membrane MTEP60 has a much more porous surface.

On the other hand, as a basis parameter in membrane formation process, viscosity also influences the thickness of the prepared flat membranes.<sup>35</sup> In this study, all microporous membranes were cast with the same casting knife, that is, with a gap of 380  $\mu\text{m}$ . However, as shown in Table IV, the membrane thicknesses, which are inversely proportional to the viscosities of PVDF casting solutions follow the trend of MTMP60 > MTEP60 > MTCP60 > MTBP60. A membrane with a thickness of  $235 \pm 0.6$   $\mu\text{m}$ , obtained with TBP–DMAc as a solvent (MTBP60), is the thinnest of the four. In this case, because of the weak solvent power and the high solution viscosity, much solvent is solidified in the three dimensional polymer chains fibriform network of gelation, and during the evaporation process (30 s), the solvent solidified in the membrane will volatilize to the air, the polymer chains of fibriform network shrinks for the action of flexibility shrinkage energy; this causes the serious shrinkage of the prepared membrane. The serious shrinkage of the prepared membrane results in dense and wizened surface.<sup>18</sup> The thickness of the membrane cast with TCP–DMAc as a solvent is  $280 \pm 0.4$   $\mu\text{m}$ , and the other two membranes cast with TEP–DMAc and TMP–DMAc as solvent are  $297 \pm 0.6$   $\mu\text{m}$  and  $330 \pm 0.5$   $\mu\text{m}$  thick, respectively. Less shrinkage is caused by a smaller lost of the solvent before phase inversion is completed.

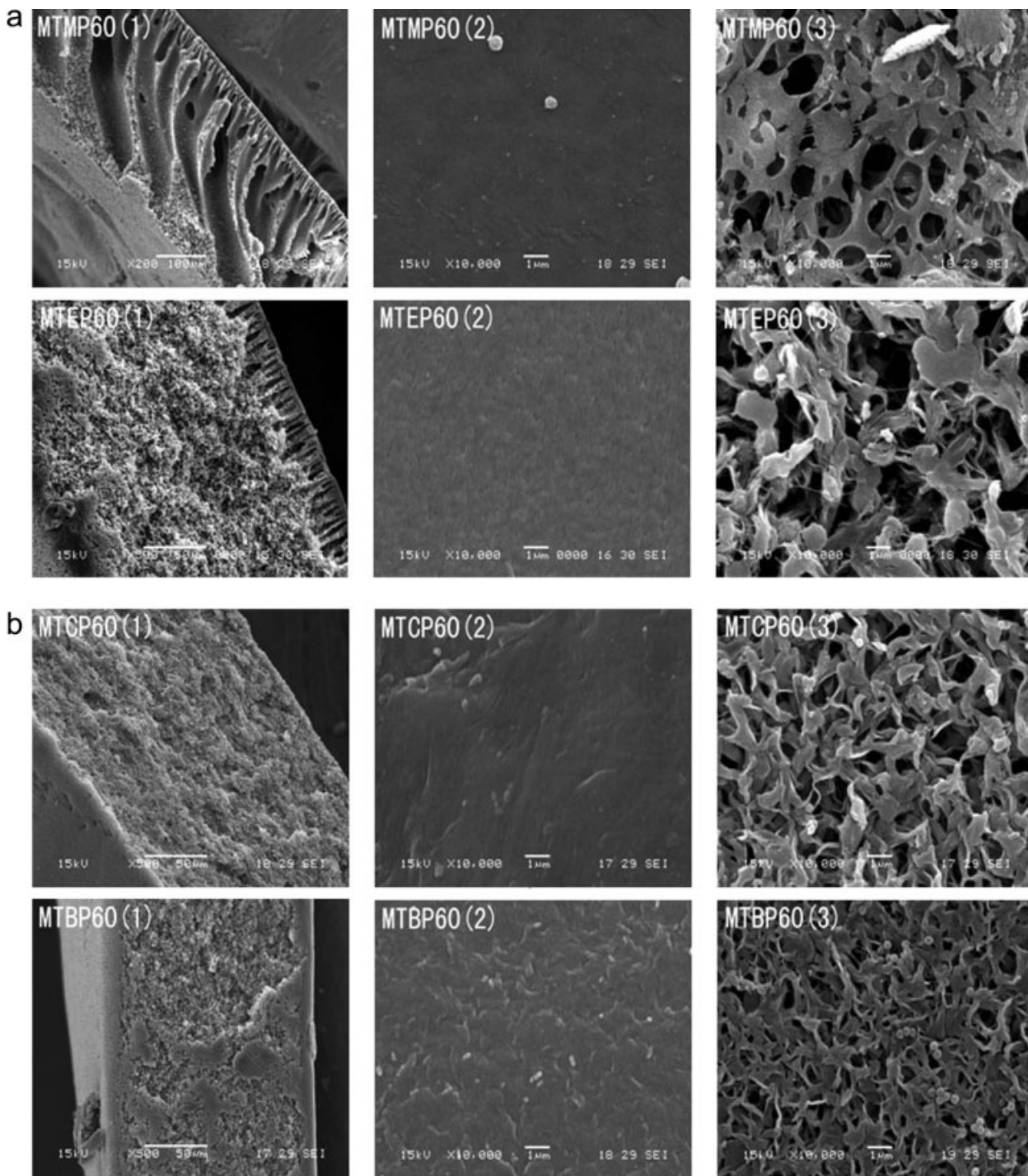


**Figure 4** SEM pictures of PVDF microporous membranes prepared by casting solutions with different phosphate–DMAC mixed solvent; 1 (cross-section), 2 (top surface), 3 (bottom surface); a (SEM pictures of MTMP60 and MTEP60), b (SEM pictures of MTCP60 and MTBP60).

The performances of the PVDF microporous membranes cast with different mixed solvent in terms of pure water flux, porosity, and mean pore radius are also listed in Table III. They are all found to follow the trend of MTMP60 > MTEP60 > MTCP60 > MTBP60. In a word, the weaker solvent power of solvent TCP and TBP leads to a larger shrinkage of

**TABLE V**  
Mechanical Strength of MTMP60 and MTEP60

Membrane	Tensile strength (MPa)	Elongation ratio (%)
MTMP60	0.47 ± 0.11	10.26 ± 0.46
MTEP60	1.33 ± 0.13	96.61 ± 0.41



TABLE VI  
Properties of Different Commercial PVDFs

Membrane	Polymer type	PVDF $M_w$	PVDF $M_n$	PVDF melt viscosity ( $\times 10^{-5}$ cp)	PVDF density ( $\text{g}/\text{cm}^3$ )	PVDF melting point ( $^{\circ}\text{C}$ )	PVDF water absorption (%)	Casting solution viscosity (cp)
MTEP60	Homopolymer	243,000	79,000	29	1.78	172	0.04	$7310 \pm 46$
MTEP60-A	Homopolymer	600,000	380,000	28	1.77	172	0.04	$4700 \pm 40$
MTEP60-B	Homopolymer	370,000	150,000	26	1.78	172	0.04	$920 \pm 33$
MTEP60-C	Homopolymer	250,000	136,000	19	1.78	168	0.03	$900 \pm 35$
MTEP60-D	PVDF-HFP Copolymer	470,000	155,000	25	1.78	142	0.03	$660 \pm 34$

the membrane, resulting in a denser and widened surface and decreasing the membrane mean pore size; the higher viscosities of casting solution with TCP and TBP as solvent, which decrease the precipitation rate during immersion process, impede the growing of macrovoids. Therefore, for MTCP60 and MTBP60, the porosity and the membrane flux decrease significantly. In addition, although the flux of MTEP60 is lower than that of MTMP60, the rejection of the former ( $90.1\% \pm 0.4\%$ ) is much higher than that of the latter ( $73.8\% \pm 0.3\%$ ) due to the decrease in the macrovoids and the increase in the denseness of membrane surface.

As mentioned earlier, of the four solvents, TMP (60 wt %)-DMAc (40 wt %) (MTMP60) and TEP (60 wt %)-DMAc (40 wt %) (MTEP60) demonstrate the stronger solvent power to PVDF, and the shrinkage of these prepared membranes is less. However, a great difference of mechanical property between the two membranes can be obtained due to the distinct morphologies of two membranes. In general, macrovoids are undesirable, because they cause mechanical weaknesses in the membrane.<sup>36</sup> The tensile strength and elongation ratio of two membranes are listed in Table V. For MTEP60, the tensile strength and elongation ratio are much higher ( $1.33 \pm 0.13$  MPa and  $96.61\% \pm 0.41\%$ , respectively) than those of MTMP60 ( $0.47 \pm 0.11$  MPa and  $10.26\% \pm 0.46\%$ , respectively). Compared to MTMP60, the macrovoids in the cross-section of MTEP60 are quite shorter, therefore, the mechanical strength of MTEP60 is improved greatly.

That is, MTMP60 and MTEP60 demonstrate stronger solvent power to PVDF and better membrane performances in comparison to MTCP60 and MTBP60. And compared with MTMP60, MTEP60 shows the higher rejection and the better membrane strength. Therefore, TEP (60 wt %)-DMAc (40 wt %) is used as solvent in the next section.

#### Effect of different kinds of PVDFs on membrane performance

The properties of different commercial PVDFs influence the membrane formation and the membrane

performances. Using TEP(60 wt %)-DMAc(40 wt %) as solvent, PVDF microporous membranes prepared by using different commercial polymers.

As listed in Table VI, the polymer of MTEP60-D is PVDF-HFP copolymer while the other four are PVDF homopolymers. And the measured viscosities of PVDF solutions follow the trend of MTEP60 > MTEP60-A > MTEP60-B > MTEP60-C > MTEP60-D. That is, the melt viscosities of PVDF homopolymers, which follow the order of MTEP60 > MTEP60-A > MTEP60-B > MTEP60-C, lead to the decreasing in the viscosities of PVDF solutions. And the copolymer (MTEP60-D) results in the lower viscosity of PVDF solution due to the lower melting point.

The light transmittance curves (Fig. 5) reveal that the precipitation rate increases as the viscosity of PVDF solution decreases, following the trend of MTEP60-D > MTEP60-C > MTEP60-B > MTEP60-A > MTEP60. That is, the decrease of PVDF solution viscosity accelerates the liquid-liquid demixing process, which contributes to the formation of macrovoids.

The SEM pictures (Figs. 4 and 6) indicate that the membranes prepared with different PVDFs exhibit similar cross-section morphology, characterized by a finger-like structure with sponge substrate. Whereas,

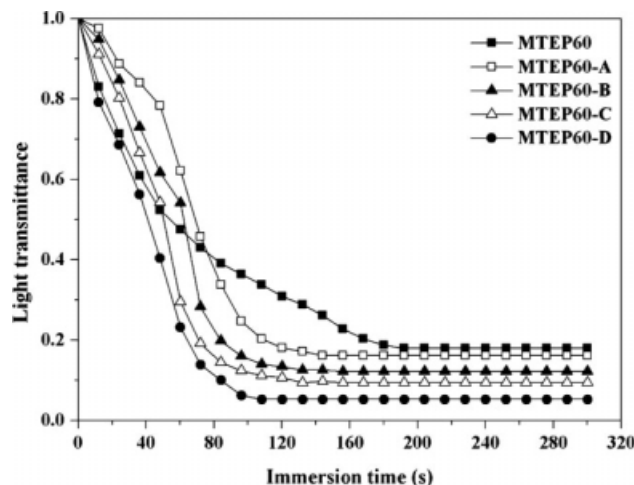
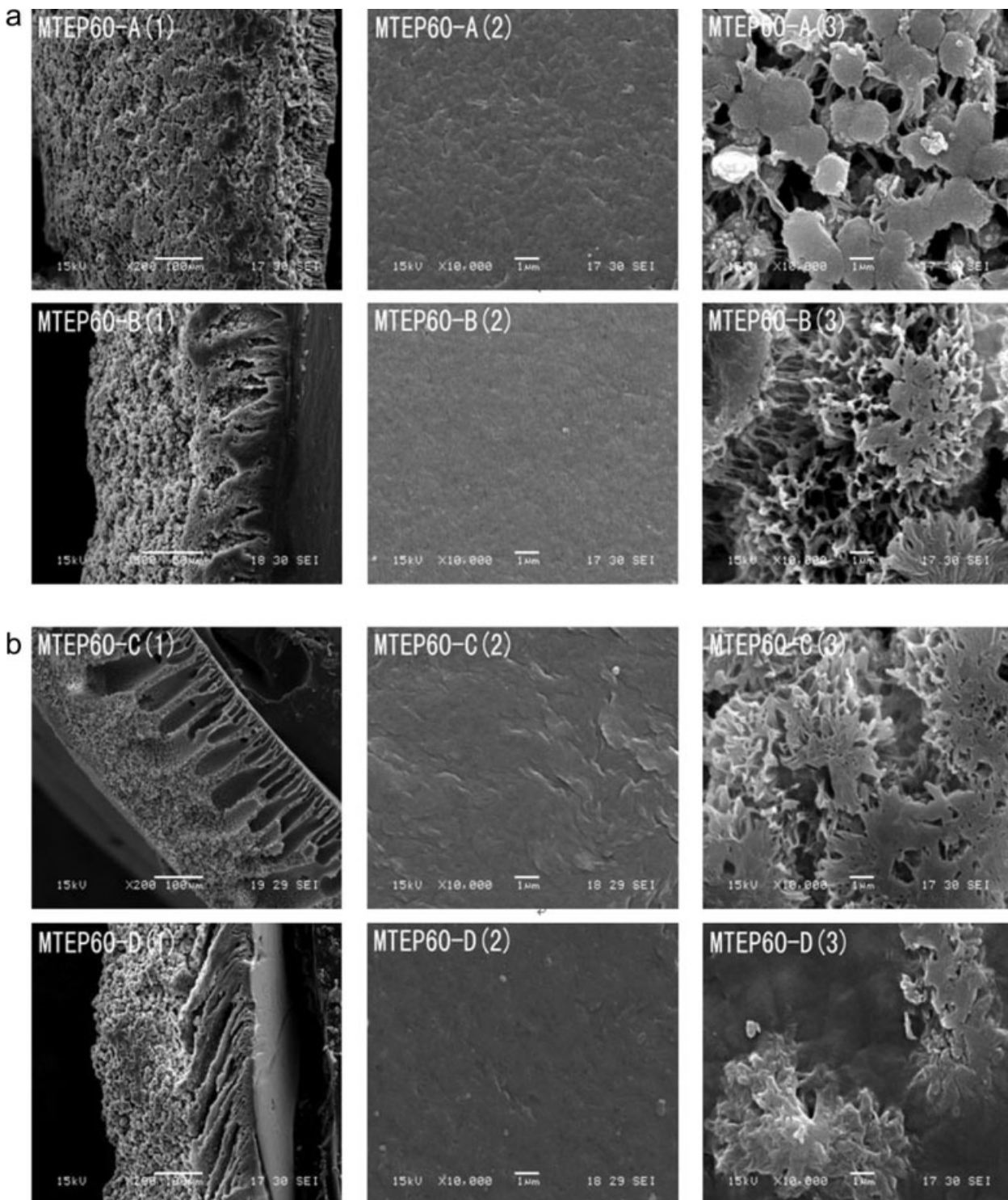


Figure 5 Light transmittance during immersion of casting solutions with different PVDFs.



**Figure 6** SEM pictures of PVDF microporous membranes prepared with different PVDFs; 1 (cross-section), 2 (top surface), 3 (bottom surface); a (SEM pictures of MTEP60-A and MTEP60-B), b (SEM pictures of MTEP60-C and MTEP60-D).

decreasing viscosity of polymer solution results in a tendency toward larger macrovoids beneath the surface, and the density of the membrane surface increases, which decreases the pore interconnectivity of the membrane; this leads to the decrease of water flux, which is shown in Table III. It should be pointed out that the porosity of the membrane

increases as the polymer solution viscosity decreases, following the trend of MTEP60-D ( $82.2\% \pm 0.3\%$ ) > MTEP60-C ( $81.4\% \pm 0.2\%$ ) > MTEP60-B ( $80.1\% \pm 0.2\%$ ) > MTEP60-A ( $77.2\% \pm 0.3\%$ ) > MTEP60 ( $76.1\% \pm 0.2\%$ ). For the membrane with lower PVDF solution viscosity (e.g. MTEP60-D in Fig. 6), longer finger-like voids extend toward the

bottom region but the pores at bottom surfaces become much smaller. Though the macrovoid structure contributes lot to the overall porosity, those dense membrane surfaces greatly lower the membrane flux.

### CONCLUSIONS

The mixed solvent, TMP–DMAc, affected the performances of the PVDF microporous membranes prepared by NIPS process. As the content of TMP in the mixed solvent reached 60 wt %, the fast precipitation rate was obtained and the resulting membrane had the high water flux of  $143.0 \pm 0.9 \text{ L m}^{-2} \text{ h}^{-1}$ . The morphologies and performances of PVDF microporous membranes with different mixed solvent systems, including TMP (60 wt %)–DMAc (40 wt %), TEP (60 wt %)–DMAc (40 wt %), TCP (60 wt %)–DMAc (40 wt %), and TBP (60 wt %)–DMAc (40 wt %) was investigated. The results showed that, the stronger solvent power of TMP–DMAc and TEP–DMAc resulted in the faster precipitation rate and the less shrinkage of the membrane; consequently, the prepared membranes demonstrated the higher flux. In addition, compared to the membrane prepared by TMP–DMAc system, the microporous membrane cast with TEP–DMAc as mixed solvent showed much shorter macrovoids beneath the skin layer, contributing to the higher rejection of  $90.1\% \pm 0.4\%$  and the much better mechanical properties of  $1.33 \pm 0.13 \text{ MPa}$  tensile strength and  $96.61\% \pm 0.41\%$  elongation ratio. The properties of PVDFs slightly influenced the cross-section morphology while greatly affected the viscosity of the PVDF casting solution. The decreasing in the melt viscosities of PVDF homopolymers decreased the viscosities of the casting solutions. Precipitation rate increased due to the decrease of PVDF solution viscosity. The formation of longer finger-like voids, which was caused by the faster precipitation process, contributed to the higher porosity, but the denser membrane surfaces obtained lowered the membrane flux.

### References

- Li, J. F.; Xu, Z. L.; Yang, H. *Polym Adv Technol* 2008, 19, 251.
- Seiler, D. A. In *Modern Fluoropolymers*; Scheirs, J., Ed.; Wiley: New York, 1997.
- Zhang, M.; Zhang, A. Q.; Zhu, B. K.; Du, C. H.; Xu, Y. Y. *J Membr Sci* 2008, 319, 169.
- Iojoiu, C.; Chabert, F.; Marechal, M.; Kissi, N. El; Guindet, J.; Sanchez, J. Y. *J Power Sources* 2006, 153, 198.
- Humphrey, J.; Amin-Sanayei, R. In *Vinylidene Fluoride Polymers*; Mark, H., Ed.; Wiley: New York, 2003.
- Ameduri, B.; Boutevin, B. *Well-architected Fluoropolymers: Synthesis, Properties, and Applications*; ENSCM; Elsevier: Amsterdam, 2004.
- Peng, M.; Li, M. B.; Wu, L. J.; Zheng, Q.; Chen, Y.; Gu, W. F. *J Appl Polym Sci* 2005, 98, 1358.
- Lin, D. J.; Chang, L. C.; Chang, C. L.; Chen, T. C.; Cheng, L. P. *J Polym Sci Part B: Polym Phys* 2004, 42, 830.
- Roy, C. C.; Chowdhury, G.; Matsuura, T. *J Appl Polym Sci* 1997, 65, 55.
- Bottino, A.; Camera, R. G.; Capannelli, G.; Munari, S. *J Membr Sci* 1991, 57, 1.
- Bonyadi, S.; Chung, T. S.; Rajagopalan, R. *AIChE J* 2009, 55, 828.
- Yeow, L. M.; Liu, Y. T.; Li, K. *J Appl Polym Sci* 2004, 92, 1782.
- Bonyadi, S.; Chung, T. S. *J Membr Sci* 2009, 331, 66.
- Buonomenna, M. G.; Macchi, P. *Eur Polym J* 2007, 43, 1557.
- Lin, D. J.; Chang, C. L. *Polymer* 2003, 44, 413.
- Cheng, L. P. *Macromolecules* 1999, 32, 6668.
- Fontananova, E.; Jansen, J. C. *Desalination* 2006, 192, 190.
- Wang, X. Y.; Zhang, L.; Sun, D. H.; An, Q. F.; Chen, H. L. *J Appl Polym Sci* 2008, 110, 1656.
- Elashmawi, I. S. *Mater Chem Phys* 2008, 107, 96.
- Benz, M.; Euler, W. B.; Gregory, O. J. *Macromolecules* 2002, 35, 2682.
- Zhao, Y. H.; Qian, Y. L.; Zhu, B. K.; Xu, Y. Y. *J Membr Sci* 2008, 310, 567.
- Seol, W. H.; Lee, Y. M.; Park, J. K. *J Power Sources* 2007, 170, 191.
- Lin, D. J.; Beltsios, K.; Young, T. H.; Jeng, Y. S.; Cheng, L. P. *J Membr Sci* 2006, 274, 64.
- Li, X. F.; Wang, Y. G.; Lu, X. L.; Xiao, C. F. *J Membr Sci* 2008, 320, 477.
- Feng, C. S.; Shi, B. L.; Li, G. M.; Wu, Y. L. *J Membr Sci* 2004, 237, 15.
- Hansen, C. M. *Prog Org Coat* 2004, 51, 77.
- Hildebrand, J. H.; Scott, R. L. *Solubility of Nonelectrolytes*, 3rd ed.; Reinhold: New York, 1950.
- Hildebrand, J. H.; Scott, R. L. *Regular Solutions*; Prentice-Hall: Englewood Cliffs, NJ, 1962.
- Segarceanu, O.; Leca, M. *Prog Org Coat* 1997, 31, 307.
- Barton, B. F.; Reeve, J. L.; Mchugh, A. J. *J Polym Sci Part B: Polym Phys* 1997, 35, 569.
- Hansen, C. M. *Prog Org Coat* 2004, 51, 109.
- Bottino, A.; Capannelli, G.; Munari, S.; Turturro, A. *J Pol Sci Part B: Polym Phys* 1988, 26, 785.
- Brandrup, J.; Immergut, E. H. *Polymer Handbook*, 3rd ed.; Wiley-Interscience: New York, 1989.
- Minagawa, M.; Takasu, T.; Morita, T.; Shirai, H.; Fujikura, Y. *Polymer* 1996, 37, 463.
- Yeow, M. L. *J Appl Polym Sci* 2003, 90, 2150.
- Vanden Witte, P.; Dijkstra, P. J.; Vanden Berg, J. W. A.; Feijen, J. *J Membr Sci* 1996, 117, 1.